Journal of Alloys and Compounds 509 (2011) 518–522

Contents lists available at ScienceDirect

Journal of Alloys and Compounds

journal homepage: www.elsevier.com/locate/jallcom

High-temperature surface alloying of nanocrystalline nickel produced by surface mechanical attrition treatment

Wei Li [a,b,*], Ping Liu [a], Fengcang Ma [a], Xinkuan Liu [a], Yonghua Rong [b]

[a] School of Materials Science and Engineering, University of Shanghai for Science and Technology, Shanghai 200093, China
[b] School of Materials Science and Engineering, Shanghai Jiao Tong University, Shanghai 200240, China

ARTICLE INFO

Article history:
Received 28 May 2010
Received in revised form
14 September 2010
Accepted 18 September 2010
Available online 25 September 2010

Keywords:
Surface mechanical attrition treatment
Nanocrystalline materials
Surface alloying
Diffusion
Characterization

ABSTRACT

A nanocrystalline surface layer is synthesized in Ni by surface mechanical attrition treatment (SMAT). The characterization of microstructure and composition indicates that foreign elements from hardened balls can permeate and diffuse into the surface layer during SMAT, which can further diffuse and homogenize in the surface layer when annealing at high temperature, leading to formation of new alloy. Foreign elements permeating into the surface layer during SMAT followed by diffusing and homogenizing at high temperature provide an alternative effective technology for surface modification.

1. Introduction

Surface nanocrystallization provides an important method to modify surface physical, chemical and mechanical properties by introducing nanostructure into the surface region of bulk materials [1,2]. Surface mechanical attrition treatment (SMAT), as an alternative technique of surface nanocrystallization, has been developed to produce bulk nanocrystalline surface layer with the gradient distribution of grain sizes along the deformation depth [3,4]. The basic principle of SMAT is the generation of plastic deformation in the surface layer of a bulk material by means of repeated multidirectional impacts of the hardened steel balls. The plastic deformation with high strain rate results in a progressive refinement of coarse grains into a nanometer scale in the surface layer. This technique has been successfully applied in achieving surface nanocrystallization and enhancing surface properties in a variety of pure metals and alloys [5–9].

Nanocrystalline surface layers produced by SMAT exhibit excellent diffusion diffusivities for foreign elements, such as nitrogen [10], chromium [11] and nickel [12], etc. For example, Wang et al. [12] reported that the effective diffusivity of Ni in the top 10 μm surface layer of Cu subjected by SMAT is more than 2 orders of magnitude higher than that along conventional high-angle grain boundaries in Cu with similar purity. Furthermore, Wu et al. [13] reported that Fe element could even diffuse from the hardened steel balls into the Co matrix during the course of SMAT and form an intermetallic compound, suggesting that SMAT is an effective method for surface modification. In our previous work [14], Fe and Cr elements in the hardened steel balls were also found to diffuse into the Fe–30 wt.%Ni alloy during SMAT and lead to the composition change of nanocrystalline surface layer, which increased the starting temperature of the reverse martensitic transformation. It is worth noting that the elements transfer from impacting balls may be harmful to the surface property of some materials [15]. These findings suggest that foreign elements can permeate into the treated surface during high-rate plastic deformation of SMAT. To our knowledge, however, the effect of annealing process on the further diffusion of foreign elements permeated into the nanocrystalline surface and its influence on the composition and structure of surface layer have not been investigated, which is of great importance to the application of surface modification for SMAT. Based

* Corresponding author at: School of Materials Science and Engineering, University of Shanghai for Science and Technology, 516 Jun Gong Road, Shanghai 200093, China. Tel.: +86 21 55271682; fax: +86 21 55271682.
E-mail address: liwei176@usst.edu.cn (W. Li).

0925-8388/$ – see front matter © 2010 Elsevier B.V. All rights reserved.
doi:10.1016/j.jallcom.2010.09.088

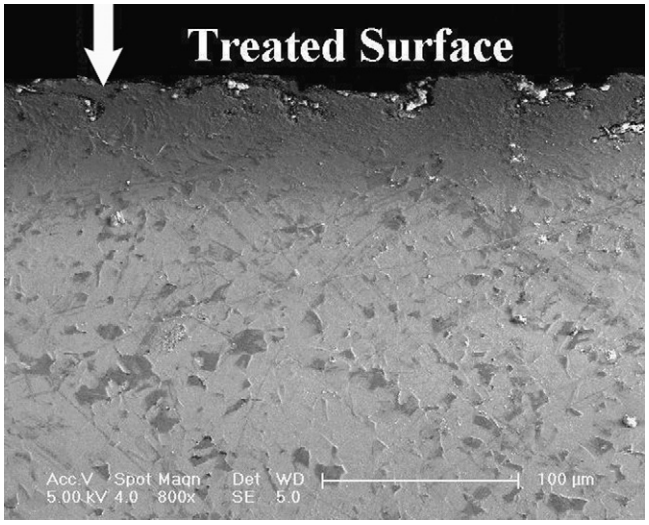

Fig. 1. SEM image of a cross-section of Ni sample after SMAT for 60 min.

on this idea, the pure Ni is selected for SMAT by using hardened steel balls composed of Fe, Cr elements and subsequently annealed at different temperatures in this work. The effect of annealing on diffused surface layer will be investigated.

2. Experimental

A plate (80 mm × 80 mm × 8 mm) of pure Ni (≥99.96 wt.%) was annealed at 973 K for 60 min and water-quenched to obtain the homogeneous coarse grains with the grain size of 10–40 μm, and then suffered from SMAT. The SMAT set-up and processing are identical to those described in Ref. [4]. In brief, the hardened steel balls were placed at the bottom of a cylinder-shaped vacuum chamber attached to a vibration generator. Because of the high vibration frequency of the system, the sample surface was struck repetitively by a large number of balls, resulting in a progressive refinement of coarse grains into the nanometer scale. In this work, the plate was treated for 60 min at a vibrating frequency of 50 Hz. The hardened steel balls have a diameter of 8 mm and a nominal composition (wt.%) of 13.00Cr, 0.15C, balance Fe.

X-ray diffraction (XRD) analysis was carried out on a D/max-2550 X-ray diffractometer (18 kW) with Cu Kα radiation. The instrumental correction was made by using the powder pattern of a Si standard and Stokes correction procedure [16]. The microstructural parameters, such as the average crystallite size, root mean square (r.m.s.) microstrain and average dislocation density, have been evaluated by the modified Warren–Averbach method by many researchers [17–19]. In this investigation, the average crystallite size, r.m.s. microstrain of nanocrystalline Ni sample were evaluated by modified single-peak Fourier analysis method suggested in our previous paper [20].

The microstructure and composition were characterized by JEM-100CX transmission electron microscopy (TEM) and JEM-2100F high-resolution TEM (HRTEM) microscopes, and JSM-6460 scanning electron microscopy (SEM) equipped with an EDS. The TEM foils were cut by using an electro-spark cutting machine and thinned by mechanical polishing from the untreated side followed by argon ion milling.

3. Results and discussion

Fig. 1 shows a cross-sectional SEM observation of Ni sample after SMAT for 60 min. It can be seen that microstructure morphology of the treated layer differs from that of the matrix. The original coarse grains in the surface layer are severely refined into ultrafine-grained structure, in which grain boundaries could not be identified. The microstructures in the treated layer change gradually from ultrafine-grained structure in the surface layer to the undeformed and polygonal grains with the grain size of 10–40 μm in the matrix. The whole thickness of the deformed layer is about 50 μm.

Fig. 2 shows the XRD profiles of the surface layers in the water-quenched and SMA-treated Ni samples. It is obvious that both samples consist of only fcc (face-centered cubic) Ni phase, suggesting no formation of new phase during SMAT process. From Fig. 2, it can be seen the shape of the profile for the treated Ni sample is different from that for the water-quenched one. According to our previous research results [7,20], it can be attributed to grain refinement and presence of a high level of microstrain. The 1 1 1 reflection was selected to determine the average crystallite size and r.m.s. microstrain. After SMAT for 60 min, the values of average crystallite size and r.m.s. microstrain are determined to be 9 nm and 5.5×10^{-3} respectively, indicating SMAT is an effective method to produce nanocrystalline structure in the surface layer.

The TEM micrographs of the topmost layer in the treated Ni sample are demonstrated in Fig. 3. Fig. 3(a) is a bright field image and shows that the sample consists of nanosized grains. The dark field image of Fig. 3(b) clearly shows that the grains are roughly equiaxed with average size of about 8 nm, which is well consistent with the XRD result (9 nm).

Normally, the grain size of nanocrystalline materials processed by severe plastic deformation (SPD) determined by TEM image is larger than that by XRD [21]. During SPD process, the dislocations formed in the grain interiors can arrange into dislocation cell boundaries to minimize their strain-energy [22]. Therefore, subgrains will create inside the original grains, which are separated by low-angle grain boundary with small misorientation. The conventional TEM image cannot differentiate these subgrains, usually displaying a whole large grain featured by high-angle grain boundary. In contrast, XRD is able to distinguish these subgrains with small misorientation [21], even less than 1–2°, and therefore gives the average size of dislocation cells or subgrains. Namely, a grain displayed in conventional TEM image may consist of several subgrains, which can be recognized by XRD [23,24]. However, in this investigation, the TEM and XRD results show that the average grain sizes are only about 8 and 9 nm. With such small grain size, dislocations can hardly exist in the interior of grains. Therefore, the grain size determined from TEM image can be very close to the average crystallite size measured from XRD.

Fig. 3(c) shows the corresponding selected-area electron diffraction (SAED) rings. It can be seen that these grains are characterized by complicated crystal structure, rather than simple fcc structure for nanocrystalline Ni, which suggests that the composition in the topmost layer changes. In order to further investigate the composition deviation phenomenon, microstructure and composition in the topmost surface and cross-section for the treated Ni sample have been determined and analyzed.

Fig. 4 indicates the microstructure and composition in the nanocrystalline Ni sample after SMAT for 60 min. Fig. 4(a) shows the HRTEM morphology of a nanocrystalline grain with a size of about

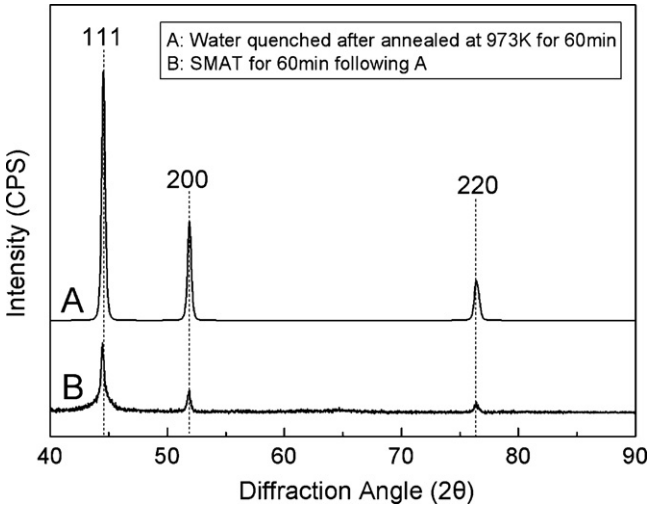

Fig. 2. XRD profiles of Ni before and after SMAT for 60 min.

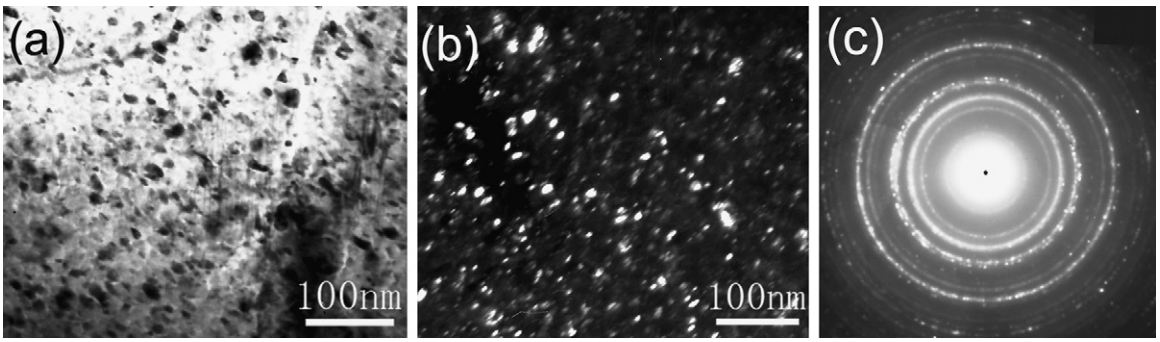

Fig. 3. Microstructure of the topmost surface layer in Ni after SMAT for 60 min: (a) bright-field, (b) dark-field image and (c) diffraction pattern.

20 nm in the topmost layer. The local EDS result of this nanometer grain is presented in Fig. 4(b), suggesting this grain is not only composed of Ni, but high content of Fe and Cr as well. The quantitative analysis results, as inserted in Fig. 4(b), indicate that the components (wt.%) are: 80.93%Fe, 11.79%Ni and 7.28%Cr, suggesting that Fe and Cr elements in the hardened steel balls diffuse into the surface layer of Ni sample. Similar phenomenon was also observed in the processing of nanocrystalline Fe–30 wt.%Ni alloy by SMAT [14]. Fig. 4(c) shows the cross-sectional morphology of Ni sample after SMAT, in which some dark regions can be observed in the surface layer. The components (wt.%) of the region marked by a white box analyzed by EDS are 77.56%Fe, 14.32%Ni and 8.12%Cr, as shown in Fig. 4(d), revealing the mixed powders from Ni sample and hardened balls may be pressed into the surface layer.

During early impingement in the course of SMAT, the powders can fall from the hardened balls and the relatively soft Ni can also be abraded by hardened balls [25]. The mixed powders of Ni sample and hardened balls can be deposited on the treated surface through the manner like cold welding. As SMAT proceeds, these powders can be pressed in the soft metallic surface layer through micro-fracture [26], as shown in Fig. 4(c), resulting in the concentrated distribution of powders in the treated surface. It can also be seen from Fig. 1 that some gray substance was coated on the part region of treated surface and some substance was pressed in the surface layer. In our previous investigation, Fe and Cr elements in hardened steel balls can also diffuse into the Fe–Ni alloy during SMAT [14]. However, the powder-pressed phenomenon has not been observed. The reason probably lies that Fe–Ni alloy is

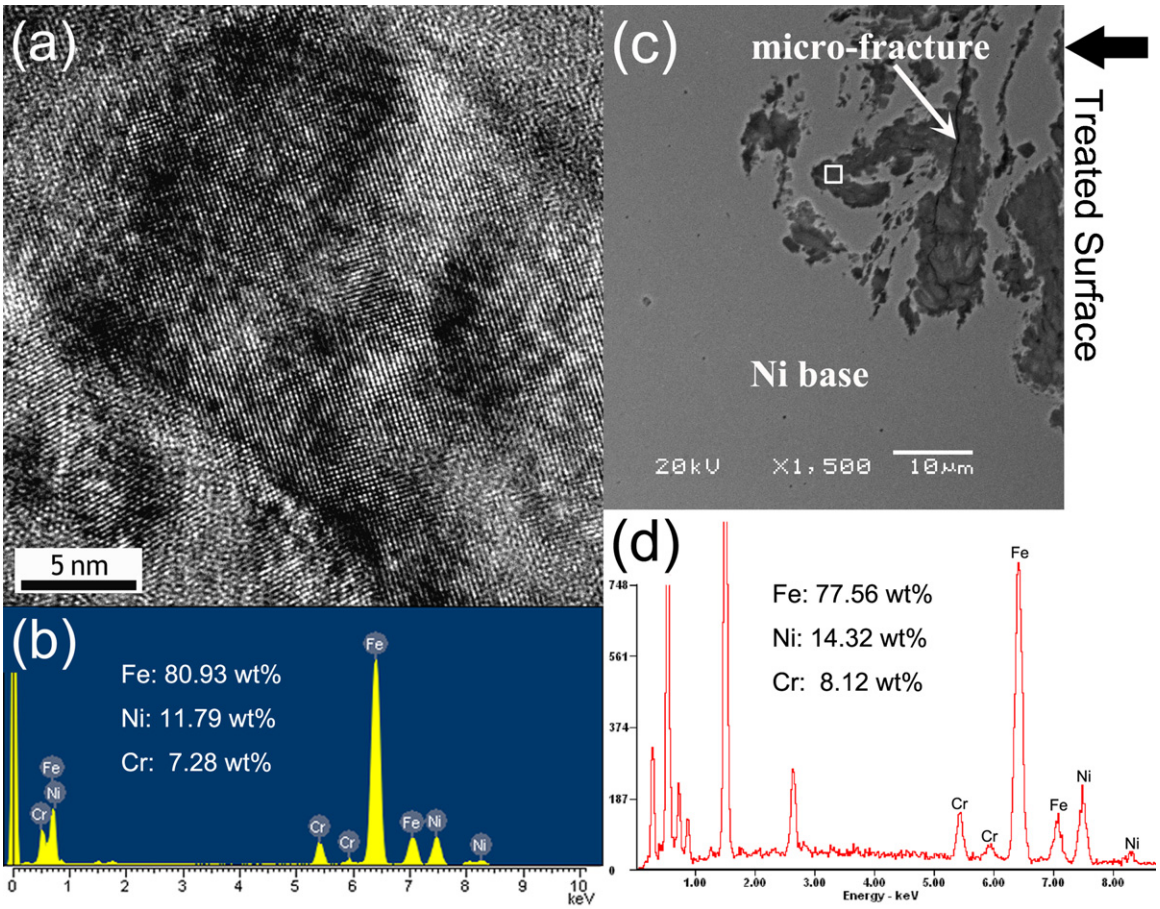

Fig. 4. Microstructure and composition in Ni after SMAT for 60 min: (a) HRTEM of nanocrystalline grain in the topmost surface, (b) EDS result of the grain in (a), (c) SEM image of the cross-section and (d) EDS result of dark area in (c) (marked by a white box).

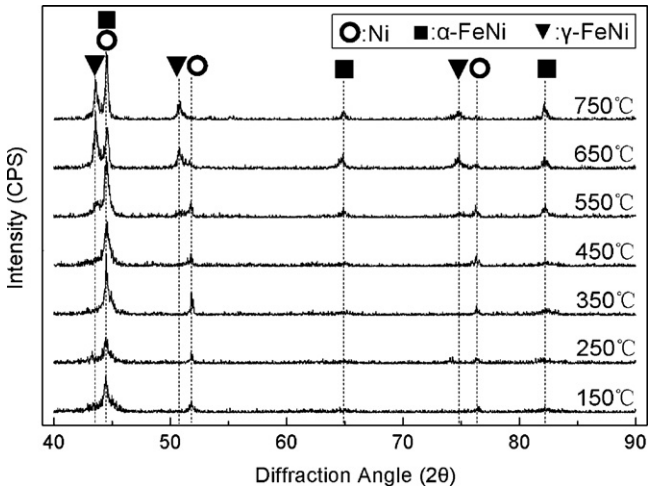

Fig. 5. XRD profiles of treated Ni after annealed at different temperatures for 30 min.

harder than Ni metal and the hardened steel powders cannot be pressed into the hard surface, only can permeate into the surface through diffusion. Based on Figs. 1 and 4(c), the maximum thickness of the pressed powders can be about 40 μm, much deeper than diffusion distance of 2 μm in Fe–Ni alloy. It is worth noting that, from Figs. 1 and 4(c), not all the surface areas are coated with powders and some powders are pressed deeply into the subsurface. Therefore, XRD profile of treated Ni sample in Fig. 2 only shows Ni phase.

Besides the press-in mode of powders, which is the primary way of the elements permeation into Ni surface, there are other possible manners through which heterogeneous elements in steel balls diffuse into the surface layer during SMAT. Firstly, high number density of grain boundaries and triple junctions in nanocrystalline Ni surface layer can provide rapid mass transport paths of Fe and Cr elements [27,28]. Secondly, for nanocrystalline materials processed by SPD, high density of dislocations can locate at grain boundaries, which provides other important channels for diffusion [29]. The average dislocation density of Ni after SMAT for 60 min was measured by X-ray diffraction peak profile analysis as high as $(7.6 \pm 0.7) \times 10^{15}\ m^{-2}$ [30]. Such high density of dislocations can remarkably accelerate the diffusion. Finally, during the course of SMAT, dislocation movement with pumping solute, increased mobile vacancy concentration and local temperature rise can also be partially responsible for the diffusion of Fe and Cr elements [13].

Since the foreign elements in steel balls can permeate into the surface layer of Ni sample during SMAT, the annealing effect on Ni surface layer should be considered. To this end, the treated Ni samples are vacuum-annealed at different temperatures for 30 min and subsequently water-quenched. The XRD profiles for Ni annealed samples are shown in Fig. 5. It can be seen that, with the increase of annealing temperature, Ni reflections gradually weaken and Fe–Ni reflections appear. Fe–Ni reflections can be clearly observed from XRD profile when annealing at 550 °C, while Ni reflections basically disappear at 650 °C. When annealing at 750 °C, XRD profile cannot detect Ni phase and presents only austenite and martensite phases of Fe–Ni alloy. These XRD results suggest that foreign elements which have been pressed and diffused into the Ni surface layer can further diffuse at high temperature, till the composition in surface layer becomes homogenized and new compound forms in the surface layer. It is worth pointing out that, due to low content of Cr element from the EDS results in Fig. 4, especially Cr content becomes lower after homogenization when annealing, its influences on Bragg angles and intensities for Fe–Ni reflections are small. Therefore, Cr element is neglected in phase analysis in Fig. 5. Actually, low content of Cr element does exist in Fe–Ni alloy.

Fig. 6 shows a typical cross-sectional microstructure of treated Ni sample after annealing at 750 °C for 30 min. It can be seen that a dark layer has formed in the surface layer after high-temperature annealing. The EDS analysis shows that the dark layer is a new FeNiCr alloy, which is consistent with XRD results. It suggests that the Fe, Cr elements indeed further diffuse and homogenize in the surface layer, and create a new alloy during annealing at high temperature. In some regions, the FeNiCr alloy is also observed to form in the subsurface layer since some powders were deeply pressed into the subsurface during SMAT. Accordingly, foreign elements permeate into the surface layer during SMAT, further diffuse and homogenize during the course of annealing, and finally form the new compound, which can provide an alternative effective technology for surface modification. The metallic materials can achieve special surface modification by selecting the milling media (hardened steel balls) containing special elements through SMAT followed annealing. It is worth noting that, however, owing to the extremely high strain rate of SMAT, it is difficult to accurately control the permeation amount of heterogeneous elements, which deserves further investigation.

It is reported that most nanocrystalline materials exhibit a remarkable resistance to grain growth, manifested by a relatively high onset temperature of grain growth (sometimes as high as $0.6T_m$, where T_m is the melting point) [31]. The T_m for pure Ni is 1726 K (1453 °C). According to the researches on grain growth kinetics of nanocrystalline Ni [32,33], the onset temperature of grain growth is about $0.3T_m$ (518 K or 245 °C). For example, Chauhan and Mohamed studied the grain growth behavior of nanocrystalline Ni prepared by electrodeposition and found that the grain size increased slowly when annealed under $0.3T_m$, while the grain size increased quickly when annealed above $0.3T_m$ [32]. Zhilyaev et al. also drew the similar conclusions when they investigated the nanocrystalline Ni produced by severe plastic deformation [33].

Annealed at different temperatures, the diffusion mechanisms of foreign elements in Ni surface layer are different. When annealed under $0.3T_m$, the grain size of nanocrystalline Ni increases slowly. High density of grain boundaries and triple junctions are still believed to be primary mass transport paths owing to the nano-scaled grain size. In addition, the dislocations can move and annihilate during subsequent low-temperature annealing process. Dislocations can pump the foreign solute atoms under dislocation

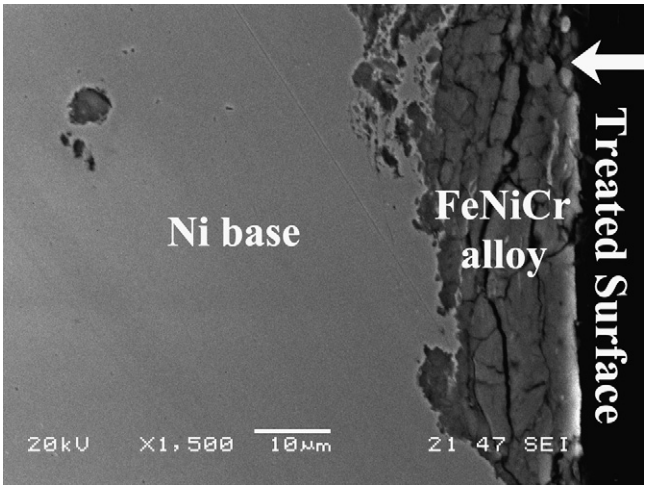

Fig. 6. SEM image of a cross-section of treated Ni sample after annealing at 750 °C for 30 min.

strain fields and move together with solute atoms [34], which is contributed to the enhanced diffusion of foreign elements. When annealed above $0.3T_m$, the grain size increases remarkably. Grain growth behavior can also influence the diffusion behavior of solute atoms. On one hand, grain growth is mostly attributed to the grain boundary migration and grain boundary is the primary channels for accommodating solute atoms. Therefore, grain boundary migration can promote the diffusion of foreign elements by carrying the solute atoms. On the other hand, based on the grain growth kinetics researches of nanocrystalline Ni synthesized by various methods, the activation energy of grain growth at high temperature for nanocrystalline Ni was determined to be close to energy for grain boundary diffusion in polycrystalline Ni (115 kJ/mol) [32,35,36]. These reports suggest that grain growth of nanocrystalline Ni involves the transport of atoms across or along the grain boundaries, which can similarly facilitate the diffusion of foreign elements.

4. Conclusions

A nanocrystalline surface layer is produced in Ni plate by SMAT. The characterization of microstructure and composition indicates that foreign elements from the hardened balls can permeate and diffuse into the surface layer during SMAT. During the course of subsequent annealing, foreign elements can further diffuse and homogenize in the surface layer, leading to the formation of new kind of alloy in the surface layer. Foreign elements permeate into the surface layer during SMAT, further diffuse and homogenize when annealing at high temperature, and finally form the new compound, which can provide an alternative effective technology for surface modification.

Acknowledgments

The present work was financially supported by the National Natural Science Foundation of China under Grant No. 50871069, “Chen Guang” project under Grant No. 09CG51 sponsored by Shanghai municipal education commission and Shanghai education development foundation, and “Selection and Training the Excellent Young College Teacher” project under Grant No. slg09015 sponsored by Shanghai municipal education commission.

References

[1] A.L. Ortiz, J.W. Tian, J.C. Villegas, L.L. Shaw, P.K. Liaw, Acta Mater. 56 (2008) 413–426.
[2] J.C. Villegas, L.L. Shaw, Acta Mater. 57 (2009) 5782–5795.
[3] K. Lu, J. Lu, J. Mater. Sci. Technol. 15 (1999) 193–197.
[4] K. Lu, J. Lu, Mater. Sci. Eng. A 375–377 (2004) 38–45.
[5] T. Hu, C.S. Wen, J. Lu, S.L. Wu, Y.C. Xin, W.J. Zhang, C.L. Chu, J.C.Y. Chung, K.W.K. Yeung, D.T.K. Kwok, P.K. Chu, J. Alloys Compd. 482 (2009) 298–301.
[6] H.L. Chan, H.H. Ruan, A.Y. Chen, J. Lu, Acta Mater. 58 (2010) 5086–5096.
[7] C.S. Wen, Z. Chen, B.X. Huang, Y.H. Rong, Metall. Mater. Trans. A 37 (2006) 1413–1421.
[8] A.L. Ortiz, J.W. Tian, L.L. Shaw, P.K. Liaw, Scripta Mater. 62 (2010) 129–132.
[9] D. Li, H.N. Chen, H. Xu, Appl. Surf. Sci. 255 (2009) 3811–3816.
[10] Y. Li, L. Wang, D.D. Zhang, L. Shen, Appl. Surf. Sci. (2010), doi:10.1016/j.apsusc.2010.08.004.
[11] Z.B. Wang, N.R. Tao, W.P. Tong, J. Lu, K. Lu, Acta Mater. 51 (2003) 4319–4329.
[12] Z.B. Wang, K. Lu, G. Wilde, S.V. Divinski, Acta Mater. 58 (2010) 2376–2386.
[13] X.L. Wu, N.R. Tao, Q.M. Wei, P. Jiang, J. Lu, K. Lu, Acta Mater. 55 (2007) 5768–5779.
[14] W. Li, X.D. Wang, Q.P. Meng, Y.H. Rong, Scripta Mater. 59 (2008) 344–347.
[15] J.W. Tian, J.C. Villegas, W. Yuan, D. Fielden, L. Shaw, P.K. Liaw, D.L. Klarstrom, Mater. Sci. Eng. A 468–470 (2007) 164–170.
[16] A.R. Stokes, Proc. Phys. Soc. 61 (1948) 382–391.
[17] A. Revesz, T. Ungar, A. Borbely, J. Lendvai, Nanostruct. Mater. 7 (1996) 779–788.
[18] T. Ungar, A. Borbely, Appl. Phys. Lett. 69 (1996) 3173–3175.
[19] T. Ungar, A. Revesz, A. Borbely, J. Appl. Crystallogr. 31 (1998) 554–558.
[20] W. Li, W.Z. Xu, X.D. Wang, Y.H. Rong, J. Alloys Compd. 474 (2009) 546–550.
[21] T. Ungar, G. Tichy, J. Gubicza, R.J. Hellmig, Powder Diffr. 20 (2005) 366–374.
[22] D.A. Hughes, N. Hansen, Acta Mater. 48 (2000) 2985–3004.
[23] T. Ungar, J. Gubicza, Kristallogr. Z. 222 (2007) 114–128.
[24] A.P. Zhilyaev, J. Gubicza, G. Nurislamova, A. Revesz, S. Surinach, M.D. Baro, T. Ungar, Phys. Stat. Sol. A 198 (2003) 263–271.
[25] A. Revesz, L. Takacs, Surf. Coat. Technol. 203 (2009) 3026–3031.
[26] A. Revesz, L. Takacs, J. Alloys Compd. 441 (2007) 111–114.
[27] R. Wurschum, S. Herth, U. Brossmann, Adv. Eng. Mater. 5 (2003) 365–372.
[28] Y. Chen, C.A. Schuh, Scripta Mater. 57 (2007) 253–256.
[29] R.Z. Valiev, R.K. Islamgaliev, I.V. Alexandrov, Prog. Mater. Sci. 45 (2000) 103–189.
[30] W. Li, P. Liu, F.C. Ma, Y.H. Rong, J. Mater. Sci. 44 (2009) 2925–2930.
[31] C.C. Koch, J. Mater. Sci. 42 (2007) 1403–1414.
[32] M. Chauhan, F.A. Mohamed, Mater. Sci. Eng. A 427 (2006) 7–15.
[33] A.P. Zhilyaev, G.V. Nurislamova, M.D. Baro, R.Z. Valiev, T.G. Langdon, Metall. Mater. Trans. A 33 (2002) 1865–1868.
[34] J. Eckert, J.C. Holzer, C.E. Krill III, W.L. Johnson, J. Appl. Phys. 73 (1993) 131–141.
[35] N. Wang, Z. Wang, K.T. Aust, U. Erb, Acta Mater. 45 (1997) 1655–1669.
[36] J. Lee, F. Zhou, K.H. Chung, N.J. Kim, E.J. Lavernia, Metall. Mater. Trans. A 32 (2001) 3109–3115.